

Full length article

Martensitic transformation and magnetic field induced effects in Ni₄₂Co₈Mn₃₉Sn₁₁ metamagnetic shape memory alloy



P. Lázpita ^{a,*}, M. Sasmaz ^{b,c}, E. Cesari ^d, J.M. Barandiarán ^{a,e}, J. Gutiérrez ^{a,e}, V.A. Chernenko ^{a,e,f}

^a University of Basque Country (UPV/EHU), 48940, Leioa, Spain

^b Firat University, 23119, Elazığ, Turkey

^c Adiyaman University, 02040, Adiyaman, Turkey

^d Universitat de les Illes Balears, 07122, Palma de Mallorca, Spain

^e BCMaterials, 48160, Derio, Spain

^f Ikerbasque, Basque Foundation for Science, 48013, Bilbao, Spain

ARTICLE INFO

Article history:

Received 30 September 2015

Received in revised form

19 February 2016

Accepted 19 February 2016

Available online xxx

Keywords:

Ni(Co)–Mn–Sn metamagnetic shape memory alloy

Martensitic transformation

Giant magnetostriction

Giant magnetoresistance

Transformation entropy

Volume effect

ABSTRACT

Transformation and multifunctional properties of a polycrystalline Ni₄₂Co₈Mn₃₉Sn₁₁ metamagnetic shape memory alloy have been investigated by extensive measurements of thermomagnetization, thermal expansion and thermoresistance under magnetic field. The martensitic transformation (MT) at zero field is near 300 K but changes moderately with field. Magnetization loops at room temperature show metamagnetic behavior and complete field-induced MT below 12 T. A non-linear phase diagram ‘*transformation temperatures versus field*’ has been established. The correlation between the transformation entropy, ΔS , with magnetic field, and temperature span between MT and Curie temperature has been also established. A transformation volume effect of about 0.45% has been estimated at MT. It has been experimentally proved that the metamagnetic effect is at the origin of the giant effects of the studied alloy, such as volume magnetostriction and magnetoresistance, which have practical importance.

© 2016 Acta Materialia Inc. Published by Elsevier Ltd. All rights reserved.

1. Introduction

Heusler NiMn-based magnetic shape memory alloys (MSMAs) are smart materials with increasing interest due to their attractive physical properties and large functional response that opens new ways for technical applications [1–7]. The martensitic transformation (MT) that these alloys undergo between the austenitic and martensitic phases is a key ingredient of all observed phenomena [8].

In the case of the well-known ferromagnetic shape memory alloys (FSMAs), like Ni–Mn–Ga ones, a strong magnetoelastic coupling is responsible for the giant magnetic field induced strain. In single crystals, the reorientation of the martensitic domains under applied magnetic field results in strains of the order of 10% [9]. During the last years the studies have been spread also towards a new class of MSMAs of composition Ni(Co)–Mn–X (X = Sn, In, Sb). These are the so-called metamagnetic shape memory alloys

(MetaMSMAs), in which the ferromagnetic austenite transforms into the weakly magnetic martensite, either ferri- or antiferromagnetic depending on the composition and/or atomic order. In these alloys MT gives rise to a large drop of the magnetization (ΔM) making these materials very sensitive to the applied magnetic field, which stabilizes the austenitic phase of high magnetization [10–12]. The magnetic field can induce a martensitic transformation below the MT temperature, T_M . This results in a number of functional properties of MetaMSMAs such as:

- Giant inverse magnetocaloric effect (IMCE): The magnetic field induces a reverse MT which, being the first order transformation, is accompanied by a heat absorption enabling cooling of the material. Particularly, IMCE has been observed near room temperature in Ni–Mn–Sn alloys, with entropy change value of 18 J/kgK at 5 T, very close to the one obtained for the prototype giant magnetocaloric Gd₅Si₂Ge₂ compound [13,14].
- Giant magnetoresistance (MR): A large MR effect of about 60%, related to the electrical resistivity abrupt change at MT, has been observed at room temperature in single crystals of Ni₅₀Mn₃₅In₁₅ alloy [15].

* Corresponding author.

E-mail address: patricia.lazpita@ehu.es (P. Lázpita).

- Metamagnetic Shape Memory Effect: The magnetic field induces the reverse MT accompanied by a full shape recovery of the sample deformed in the martensitic state. It was observed in a $\text{Ni}_{45}\text{Co}_5\text{Mn}_{36.7}\text{In}_{13.3}$ single crystal at 298 K, under an applied magnetic field of 7 T [16].

All these effects are especially interesting when appearing at room temperature.

The transformation characteristics and magnetic properties of MSMA strongly depend on their composition (see, e.g., Refs. [12,17] for FSMA). In the case of MetaMSMA several studies have reported that the addition of Co or Fe is very effective to tune their physical characteristics and functional properties, including ductility and strength [10,18–24]. Recently, a complete phase diagram of the Ni–Co–Mn–Sn MetaMSMA has been determined, establishing the dependence of the magnetostructural transition and related properties with the composition [12].

In the present work, we perform an extensive study of the influence of magnetic field on the transformation behavior and related giant magnetostriction and magnetoresistance effects, in the $\text{Ni}_{42}\text{Co}_8\text{Mn}_{39}\text{Sn}_{11}$ MetaMSMA. This alloy was chosen as a model for such exhaustive measurements due the highly pronounced metamagnetic features and the close proximity to room temperature of the martensitic transformation that makes this alloy very interesting for technical applications.

2. Experimental

An ingot of $\text{Ni}_{42}\text{Co}_8\text{Mn}_{39}\text{Sn}_{11}$ was prepared by the multiple arc melting, heat treated at 1170 K during 14 days and water quenched. The samples used for this study were spark-cut from the ingot, heat treated at 1070 K during 30 min in argon and quenched into cold water. The composition of the sample was determined by energy dispersive X-ray spectrometry (EDXS) using a TM300 table top SEM from Hitachi. A Bruker D8 Advance X-ray diffractometer equipped with a Cu tube was used to characterize the structure at room temperature using the FullProf software for data treatment [25]. The martensitic and magnetic transformation temperatures were determined with a differential scanning calorimeter running from 173 K to 473 K and temperature rate of ± 5 K/min. Magnetization loops and thermomagnetization curves were studied in a vibrating sample magnetometer (VSM) mounted in a Cryogenic Ltd. platform under applied magnetic fields up to 12 T in a range of temperatures from 150 K to 320 K. A complementary second VSM with a maximum field of 1.8 T was used to extend the temperature range of the magnetic measurements up to 450 K. Electrical DC resistance measurements as function of temperature and magnetic field up to 12 T were carried out using the four-probe technique in the Cryogenic Ltd platform. For these measurements the magnetic field was applied parallel to the measuring electrical current, and the resistance was determined by the averaging the forward and reverse voltage drops at the sample. Magnetostrain measurements were performed in samples measuring $3.5 \text{ mm} \times 5.0 \text{ mm} \times 1.5 \text{ mm}$ using two strain gauges; one was glued on the sample and the other one on a quartz plate used as reference. The sample deformation, parallel and perpendicular to the applied magnetic field, was measured as function of magnetic field up to 12 T in a temperature range between 150 K and 320 K, in the same Cryogenic Ltd platform.

3. Results and discussion

3.1. Transformation, structure and morphology

Fig. 1 shows structural and calorimetric evidence of MT in the

studied alloy. Martensitic and magnetic transformations are clearly found in DSC curves (inset to Fig. 1). The martensitic and austenitic start and finish temperatures determined by DSC are $T_{\text{ms}} = 317$ K and $T_{\text{mf}} = 286$ K and $T_{\text{as}} = 305$ K and $T_{\text{af}} = 332$ K, respectively, while the Curie temperature is 403 K. The total entropy change averaged for the forward and reverse MT is equal to $\Delta S^{\text{DSC}} = |26.5| \text{ J/kg}\cdot\text{K}$.

The XRD pattern in Fig. 1, acquired at room temperature, after a cooling process from high temperature, has been indexed as an $L2_1$ ordered structure ($Fm\bar{3}m$ space group) typical of the austenite in these alloys. Peaks of an additional FCC γ -phase are also identified. The lattice parameters determined for these two cubic phases are 6.02 Å and 3.64 Å, respectively. At this temperature, some amount of the low-symmetry martensitic phase expected from DSC results is also present. The extra reflections can be attributed to an orthorhombic phase with cell parameters $a = 4.46$ Å, $b = 5.66$ Å and $c = 4.24$ Å.

The secondary electron micrograph displayed in Fig. 2 shows the microstructure of the sample, where the presence of the dark γ -phase precipitates with typical sizes of 10 μm is clearly visible. Moreover, the image presents two black round regions (marked with an arrow in Fig. 2) associated with the sample tiny holes originated during the fabrication process. Due to the small amount of martensitic phase at room temperature the typical martensitic platelets are hardly observed in this image. The atomic composition of each phase was determined by EDX as $\text{Ni}_{42.8}\text{Co}_{6.7}\text{Mn}_{38.8}\text{Sn}_{11.7}$, for the $L2_1$ matrix, and $\text{Ni}_{39.3}\text{Co}_{17.4}\text{Mn}_{41.9}\text{Sn}_{1.4}$ for the FCC γ -phase precipitates, respectively. The precipitates are enriched in Co. They also exhibit a very low Sn content, corresponding to the FCC solid solution present in the Ni–Mn rich side of the Ni–Mn–Sn phase diagram [12]. A considerable difference in composition between $L2_1$ matrix and FCC precipitates is, probably, due to the not high enough temperature (1073 K) to dissolve the γ -phase (see also Ref. [26]). Although the high texture of the samples prevents a quantitative analysis of the different phases by X-ray diffraction, a sharp contrast between the two phases, as shown in Fig. 2, enables an estimation of about 5 vol.% of the γ -phase, when averaged through the large surface areas.

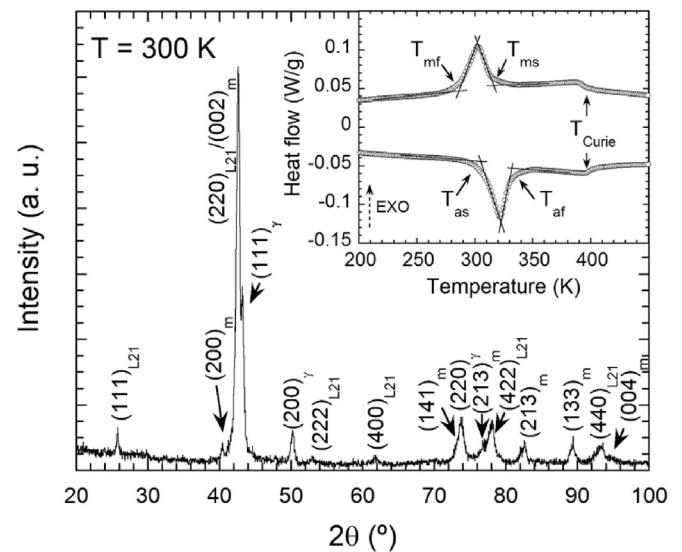


Fig. 1. X-ray diffraction pattern measured at room temperature after a cooling process from high temperature. $L2_1$, γ and m subscripts correspond to the austenitic phase, FCC- γ phase and martensitic one, respectively. The inset shows the DSC curves displaying the forward and reverse martensitic transformation and Curie temperature.

Download English Version:

<https://daneshyari.com/en/article/7878391>

Download Persian Version:

<https://daneshyari.com/article/7878391>

[Daneshyari.com](https://daneshyari.com)